LA-UR-18-29040
Approved for public release; distribution is unlimited.

Title: Nitroplasticizer-water phase diagram

Author(s): Edgar, Alexander Steven
Yang, Justine H.
Yang, Dali

Intended for: Report

Issued: 2018-10-04 (rev.1)

Nitroplasticizer-water phase diagram

Alexander Edgar, Justine Yang, Dali Yang*
Engineered Materials Group (MST-7), Materials Science and Technology Division
Los Alamos National Laboratory, Los Alamos, NM 87545, USA

Abstract: Nitroplasticizer (NP) is used in conjunction with poly(ester urethane) block co-polymer as binder material for polymer bonded explosives (PBX). Water content contributes directly to the stability of NP, poly(ester urethane), and ultimately the PBX. Therefore an NP-water miscibility phase diagram can be an important tool in understanding potential water content in NP and further PBX processes. To determine the NP-water miscibility phase diagram, a systematic series of experiments was conducted. NP samples were saturated with water and ramped through incremental temperature steps. Aliquots were taken at each step after equilibration. Water content in NP was determined by Coulmetric Karl Fischer (KF) titration at each incremental temperature step. The sample aliquots were then analyzed by Thermogravimetric analysis (TGA), Differential Scanning Calorimetry (DSC), and Transmission Fourier Transform Infrared Spectroscopy (Near-IR). The resultant data were analyzed and combined to construct an NP-water phase diagram. The phase diagram, ranging from 500 ppm to 5800 ppm water concentration and −90°C to 130°C, contains six distinct phases separated by five distinct phase separations.

1 Introduction

Nitroplasticizer (NP), a 50:50 eutectic mixture of bis-2,2-dinitropropyl acetal (BDNPA) and bis-2,2-dinitropropyl formal (BDNPF), is used in conjunction with Estane®5703 poly(ester urethane) as binder materials for the PBX-9501 formulation.[1] Molecular structures of BDNPA and BDNPF are shown in Figure 1. By using polymer binder, the composite of 1,3,5,7-tetranitro-1,3,5,7-tetrazocane (HMX) is more resistant to catastrophic insult, and can be machined into desired forms while remaining an effective explosive material.[1b] Due to the direct correlation of polymer chain length with mechanical properties of the PBX, polymer degradation rates are important for the safe use of the material.[2]

Previous studies have suggested the concentration of water in PBX systems is important for two reasons. First, excessive water allows acid formation from interaction with NP, which results in acid catalyzed hydrolysis of poly(ester urethane) and chain scission along polymer backbone[3]. Secondly, scarce water causes NP to degrade to form NO_x, which results in oxidative crosslinking/non-hydrolytic scission of poly(ester urethane).[1a, 3a, 4] Both reactions result in undesirable changes in the mechanical properties of the PBX. Due to the degradative effect of water on the polymer and NP,[1a, 3b, 4a-c] determining the water content of the PBX system is crucial. As the water absorption in both HMX and poly(ester urethane)[4c] have been studied, this paper focuses on the miscibility of water in NP, specifically constructing the NP-water phase diagram.

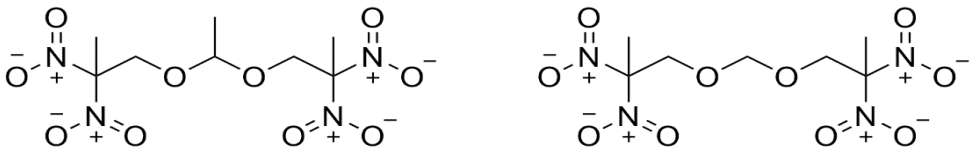

Figure 1: Chemical structures of BDNPA and BDNPF.

* Corresponding Author: Dali Yang
Phone: 505-665-4054
E-mail: dyang@lanl.gov

2 Experimental

2.1 Sample preparation

Three glass vials were loaded with 12 mL of baseline NP each. The replicate aliquots were then saturated with water by adding 10 mL deionized (DI) water to each sample and labeled: NP-A, NP-B, and NP-C. After vigorously shaking, the vials were placed in a 25°C thermal water bath overnight (16 hours), allowing the NP-water mixtures to equilibrate. Since NP has a higher density than water, the NP phase was at the bottom of the vials. To collect the NP samples at a specific temperature, 0.6 mL of sample was withdrawn using a 1 mL syringe from the bottom of the vials while they were continuously heated in the thermal bath. This procedure was performed carefully as not to contaminate the NP sample with the water phase. NP-A, NP-B, and NP-C were sampled from 25°C to 70°C at 5°C increments.

At each temperature, at least two hours were allowed for the samples to reach thermal equilibrium, with the exceptions of 25°C and 40°C, both with 16 hours of equilibration time. At each temperature, NP-A, NP-B, and NP-C were immediately analyzed using Coulmetric Karl Fischer (KF) titration, totaling 0.3 mL of NP measured at each temperature step. Following the KF titration injection, 1.5 mL mixed samples were aliquoted from NP-A, NP-B, and NP-C (0.5 mL/each) for later analysis by Thermogravimetric analysis (TGA), Differential Scanning Calorimetry (DSC), and Transmission Fourier Transform Infrared Spectroscopy (Near-FTIR).

At 70°C, 5 mL aliquots of supernatant water were taken from the top of each vial for later analysis. After the temperature ramp and sampling NP-A, NP-B, and NP-C still contained 5 mL of supernatant water and 7 mL of NP (values approximate). To quantify the nitric acid (HNO_3) concentration in the supernatant water, a set of nitric acid aqueous solutions were prepared by serial dilution of 70% HNO_3 stock solution (Fischer chemical, Pittsburgh, PA) using DI water (Fisher chemical). The concentration ranged from 70% (stock solution) to 0.1% HNO_3. The samples were prepared on a Mettler Toledo XS204 balance in a fume hood.

2.2 Karl Fischer Titration

KF measurements were taken on the C30S Coulmetric KF (Mettler Toledo, Columbus, OH). Water saturated NP samples were drawn from NP-A, NP-B, and NP-C with the method described in the Sample preparation section above. The samples were quantitated for water content in triplicate, with KF sample size totaling 0.3 mL. Prior to the KF measurements, the instrument was claibrated and the anolyte/catholyte solutions were changed out for fresh solutions (Coulomat AG and CG respectively, Honeywell, Morris Plains, NJ). Additionally, prior to each testing session calibration check standards were analyzed using a combination of three water standards of 100 ppm, 1000 ppm, and/or 10000 ppm water(Honeywell, Morris Plains, NJ).

2.3 Thermogravimetric Analysis

TGA measurements were taken on a TGA Q500 (TA Instruments, New Castle, DE). The TGA method measured mass loss at temperature (volatiles, including water). All samples were vigorously shaken to ensure uniformity. With each sample, 25 – 30 mg was loaded into an aluminum pan (on a platinum tray) and heated with a ramp rate of 5°C/min under a 10 mL/min nitrogen purge from room temperature (approximately 20°C to 25°C) to 300°C.

2.4 Near Infrared Spectroscopy

Near-IR transmittance spectroscopy measurements were taken on a Nicolet™ iS50 FTIR (Thermo Fisher, Waltham, MA). All samples were shaken vigorously before 0.5 mL was added to a quartz windowed flow cell with temperature control. Duplicate background measurements were taken prior to the sample being loaded. The samples were scanned 32 times with resolution of 4 cm^{-1}. The samples were then ramped to the temperature at which they had been sampled and the transmittance was measured. The 25°C, 55°C, and 70°C samples were ramped to 70°C in 5°C increments, allowing 5 minutes of equilibration time at each step and taking multiple measurements at each step. Additionally, the supernatant water from NP-A, NP-B, and NP-C and serial dilutions of nitric acid ranging from 70% to 0.1% HNO_3 (Appendix A) were tested in ambient temperature quartz flow cells sample containers.

2.5. Differential Scanning Calorimetry

DSC measurements were taken on a DSC Q2000 instrument (TA Instruments, New Castle, DE). A water-saturated sample of NP was added to an aluminum hermitic DSC pan with a sealed lid. The sample was tested in conventional DSC mode for thermal transitions. The sample was remade and cycled from −90°C to 80°C to −90°C with 15-minute isotherms at each temperature extreme. The method was also applied to NP-water standards (non-water saturated) to determine the change in water melt temperature with water concentration.

The water saturated DSC sample was again remade and the lid was punctured to allow water vapor to escape during the initial heat ramp of the DSC run. The sample was dried of water on the initial temperature ramp from −90°C to 110°C at 1°C/min and held at 110°C for 60 minutes to allow water to escape. The sample was then assumed ~0 ppm (water). The run was continued to determine if thermal transitions were detectable by cycling temperature from −90°C to 110°C with 15-minute isotherms at each temperature extreme.

3 Results and Discussion

3.1 Karl Fischer Titration

Prior to KF characterization, a method was developed to accurately determine the water concentration in NP. To find the optimal titration volume, volumes of the standards were varied, and determined 0.8 mL - 1 mL of the 1000 ppm standard gave the smallest percent error (0.026%). Subsequent analyses were aimed around 1 mL when measuring other standard solutions with low water concentration. To minimize waste generation, but ensure accurate measurements, the low volume limit of the NP sample was determined. A set of NP-water mixtures with different water concentrations was prepared, with concentration varying from 424 ppm to 4000 ppm. Detailed dilution procedures are documented in Appendix A.

In its natural form, NP contains a trace amount of water (<1000 ppm). Initially at room temperature, with water concentration below 2000 ppm, water and NP forms a one phase mixture. The original intent was to make a calibration curve starting from 100 ppm, however it was not possible to obtain such “dry” NP without degrading it. By placing NP in a vacuum oven at room temperature for 48 hours, the lowest water content achieved was 424±21ppm, determined by KF titration using 0.3 mL of the sample. This NP is reffered to as dry NP. Using this dry NP, an NP sample with water concentration of 1742 ppm was also made, by adding a predetermined amount of water. By changing the weight ratio of these two solutions, eight more solutions (5 mL/each) were made with the water concentration varying between 424 ppm and

1742 ppm, their water concentration determined by KF titration using 0.3 mL of solutions. The results from the KF and weight measurement agree, suggesting the sample size (0.3 mL) will give reliable water concentrations in NP samples. Detailed results and procedures using KF titration are given in Appendix B.

The results of the KF analysis of NP-A, NP-B, and NP-C show from 40°C and above, the water saturated NP samples were found to contain predictably greater concentrations of water as temperature increased. Figure 2 shows the linear least squares series of average water concentration value vs. average sampling temperature, the correlation is well fit. The raw data is given in Appendix C. However, between 25°C and 35°C (shown in Figure 2 as red squares), the coefficient of variation ranges up to 43% when averaging sample injections of triplicate or greater multiplicity. The unpredictability of the water concentration determination below 40°C indicates a heterogeneous emulsion phase of the water saturated NP. In Figure 2, the linear fit of water concentration vs. temperature indicates the NP-water mixture changes from a heterogeneous emulsion to homogeneous solution between 30°C and 40°C.

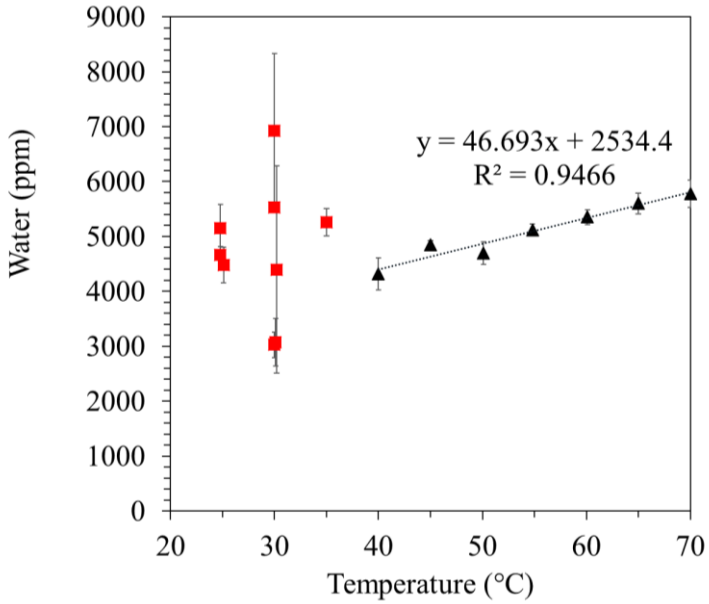

Figure 2: Coulmetric KF titration results of water saturated NP at various temperatures, error bars show sample standard deviation of up to nine sample replicates per point. Heterogeneous results shown in red, homogeneous results shown in black.

3.2 Thermogravimetric analysis

To verify the water concentration in the NP samples, TGA tests were also conducted. Figure 3 compares the weight loss of water saturated NP sampled above 40°C at two specific TGA temperatures, 100°C and 117°C. Both techniques (TGA and KF titration) do not differentiate free and bound water. One could expect the TGA results would give different concentrations than KF as TGA does not differentiate between water and other volatile compounds. The TGA reading is simply mass loss at a specific temperature.

Considering the high elevation in Los Alamos (~2300 m), the initial assumption was water would completely boil out of the NP solution around 100°C. The comparison of the weight losses of these samples at 100°C to their corresponding KF results, showed TGA results ~1000 ppm less than the KF measured water concentrations. Attempting to match the TGA

results to the KF results, the specific temperature was extended from 100°C to 117°C. This suggests some of water molecules form hydrogen bonds with NP molecules, and require more energy to phase change to water vapor. As shown in Figure 3, the lower temperature samples (below 55°C) do not conform well to the assumption water boils from NP at 117°C.

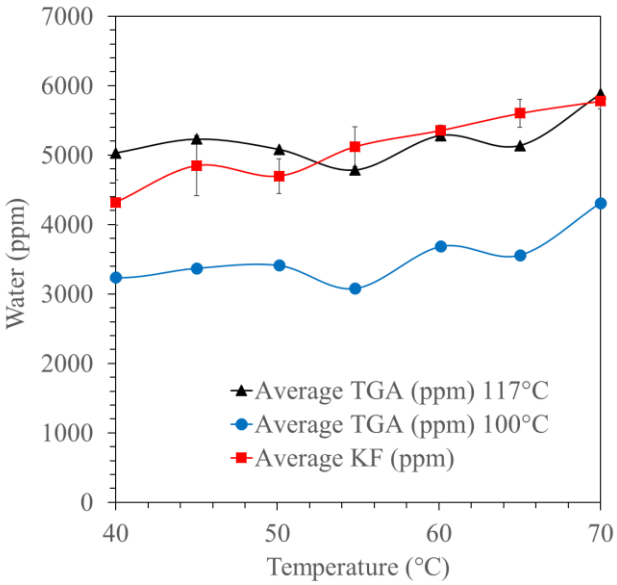

Figure 3: Sample equilibration temperature vs mass loss measured by TGA at 100°C and 117°C in water saturated NP or water concentration measured by Karl Fischer titration, error bars show sample standard deviation of triplicate KF measurements.

To water saturate NP samples, a water layer was added at the top of the NP phase, however doing so also NP saturates the water layer, refered to here as supernatent water. Earlier work suggests nitrous acid (HONO) may be present in the NP phase,[4d] and the supernatant water can extract HONO molecules from the NP phase. Due to HONO's instability, the HONO will decompose to form nitric acid (HNO_3). Therefore, a set of nitric acid serial dilutions was prepared from 70% to 0.1% HNO_3 and analyzed these solutions and DI water by TGA. The supernatant water samples were analyzed by the same TGA method to compare results, as shown Figure 4.

Figure 4 includes DI water results, at the high elevation of Los Alamos (~2300m), the water boiling temperature should measure ~91.6°C. The metric used for comparison here is maxima of first derivative of weight loss temperature (DT). The DT of DI is decreased from theoretical to 79.8°C, because of the small sample size (25 – 30 mg). The DTs of the nitric acid samples show an initial drop to 75.5°C at ~2%, reach a max of 89°C at ~10%, and level out around 15% HNO_3.

The average DT of the supernatant waters from the NP-A, NP-B, and NP-C samples is 88.9°C, which is 3.2°C higher than the DT of DI. Assuming this increased DT of the supernatant water samples is due to the presence of HNO_3, the nitric acid concentration in the supernatant water is estimated to greater than 9%. However, placing an upper limit on the estimated concentration of HNO_3 is more difficult to resolve from the TGA results as the supernatant water sample trace crosses the HNO_3 standard curve at multiple points. The pH of teh supernatent water was tested, and found to be between 2 and 4; placing the hydronium concentration between 1% and 0.01%. Both extremes fall well short of the expected pH from greater than 9% HNO_3, which should yield pH >1.05 assuming cation/anion balance. However, it is possible the TGA

reading is more sensitive to anionic nitrate (NO_3^-) than HNO_3; the observed results are consistant with the existance of an imbalance in hyronium and nitrate, specfically as more nitrate than hydronium in the supernatant water. Clearly, other analytic techniques are needed to obtain a conclusive result, and as this work does not contribute to the phase diagram of NP-water, this could be the focus of further work.

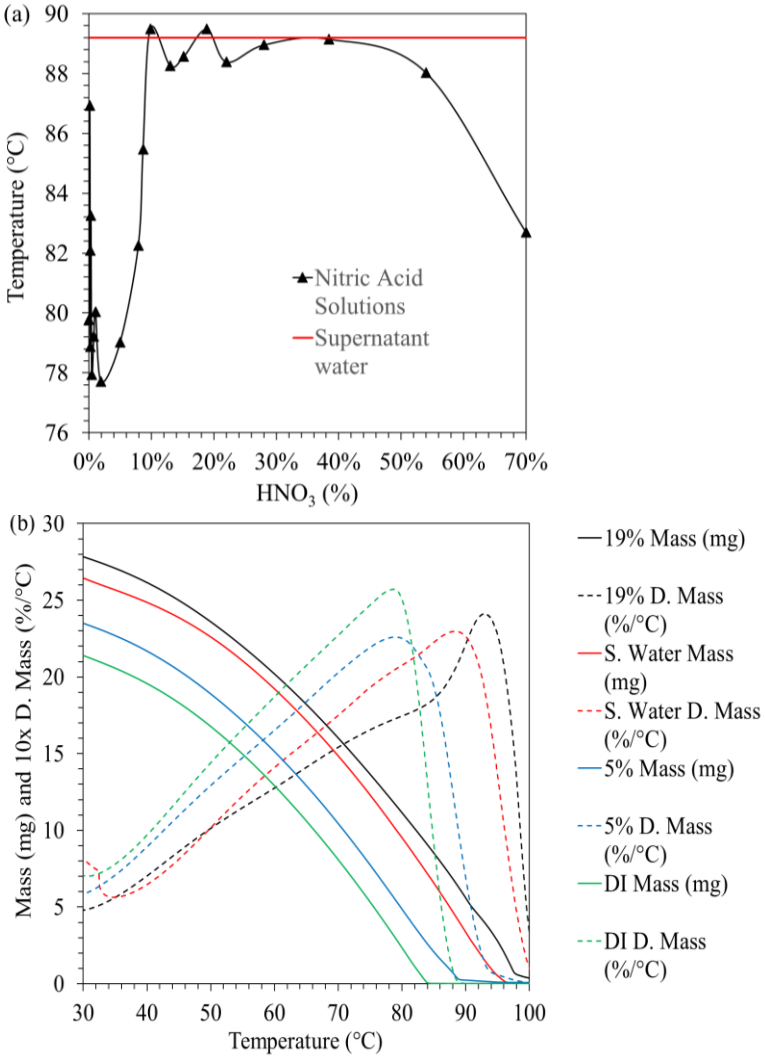

Figure 4: (a) Results comparing first derivative peak maxima of TGA of nitric acid solutions at various concentrations with TGA result of Supernatant water. (b) TGA results of select Nitric acid dilutions and DI water, mass loss is shown in solid lines; first derivative of mass loss is show in dashed lines the maxima of which were used as comparison metric.

3.3 Near-IR

As shown previously in Figure 2, water concentration increases as temperature increases. This trend becomes especially clear at temperatures above 40°C. To study how temperature affects the interaction between water and NP molecules, Near-IR analysis was conducted for the samples with different water concentrations by ramping the temperature from room temperature to 70°C in 5°C increments. One baseline NP, and two NP samples collected at 25°C and 70°C were analyzed. From the KF titration, their water concentrations are 540 ppm, 3702 ppm, and 5777 ppm, respectively.

In the Near-IR spectrum of an NP/water mixture, there are two peaks related to the water molecules. The first peak is between 5425 cm^{-1} to 4975 cm^{-1} (called 5k here) and is related to free water; the second peak is between 7200 cm^{-1} to 6500 cm^{-1} (called 7k here) and is the overlapping peaks of bound and free water.[5] Since the 5k peak is clear of interference and a relatively intense signal for the experimental conditions (Figure 5), only the results from this peak are used for the following discussion. Figure 5 presents a set of the Near-IR spectra of the baseline samples collected at the temperatures at which they were sampled. Since the baseline NP only contains ~540ppm water, the sample appears clear and does not show any phase separation. The peak intensity remains more or less the same as the temperature increases from room temperature to 70°C, suggesting the effect of temperature on the 5k peak is insignificant.

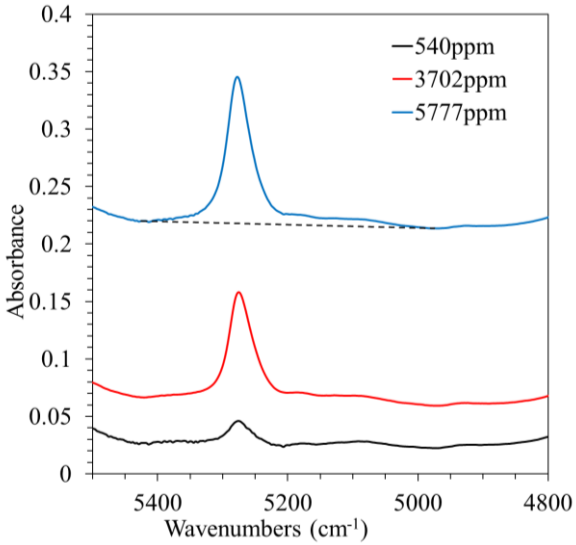

Figure 5: Shifted scale overlay of NP Near-IR signals produced at sampleing temperature (540ppm is tested at 25°C).

For the other two samples, since they were collected at 25°C and 70°C when the NP was fully saturated with water, it is expected to see a phase separation when the 70°C sample was cooled to room temperature. However, instead of forming two clearly defined completely separate phases, the appearance of the mixture changes from clear to cloudy as the temperature decreases. The water phase forms tiny droplets (<100 micrometers), which are uniformly distributed throughout the NP phase. During the Near-IR measurement, as temperature increases, the appearance of the mixture changes from cloudy to clear. To ensure representative Near-IR spectra, more than four spectra were collected from different regions at each temperature and averaged.

Figure 6 presents the integration areas of the 5k peaks for these three solutions measured at different temperatures. For the baseline NP, the intensity of 5k peak does not change significantly over the temperature range. However, the other samples show initial increase and then leveling off above specfic temperatures. The leveling temperatures for these two samples are 35°C and 50°C, respectively. Compared to their collecting temperatures, 25°C and 70°C, there is -10°C and 15°C differnces respectivly. The gap between leveling and equilibration temperature for the 70°C sample suggests NP/water forms a metastable equilibrium starting at the leveling temperature, delaying phase separation as the metastable state transitions into an equilibrium state. The 25°C gap between leveling and equilibration reenforces the idea that

saturated NP forms an emulsoin somewhere between 30°C and 40°C. This result also suggests the crash from homogenaity to emulsion state is close to 35°C with 3702 ppm water.

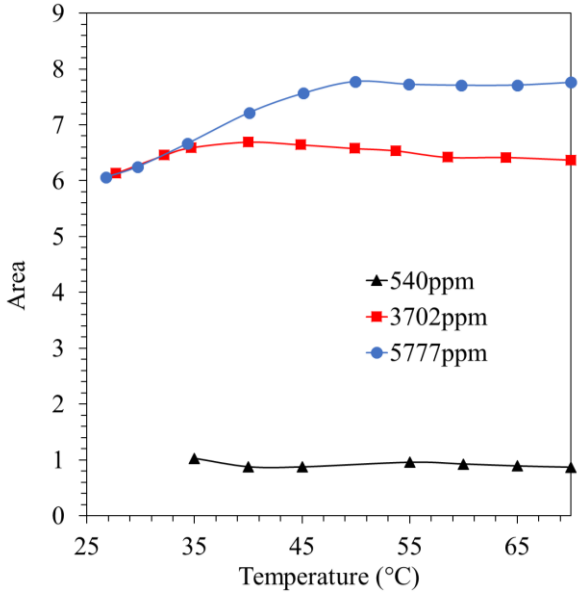

Figure 6: Area by integration from ~5425 to ~4975 wavenumbers vs flow cell temperature. The figure shows the homogeneous saturation of the NP above 50°C, evidenced by the curve leveling of the 70°C equilibrated NP sample beyond 50°C.

3.4 Differential Scanning Calorimetry

To determine low temperature phase transitions, DSC measurements were taken for NP-water samples with different water concentrations. Three samples were used in four runs, the first three runs were 540 ppm (inert NP), 1417 ppm (a prepared homogeneous standard), and 3702 ppm (room temperature water saturated NP), the fourth run was approximated to ~0 ppm. As shown in Figure 7, the NP-water runs, determined by heat-cool-heat experiments, show a clear glass transition (T_g) with an endothermic peak around −67.8°C to −67.2°C, indicating the transition of the NP from a liquid to solid material with little dependence on water concentration. Further, the three samples containing water show a melting temperature (T_m), which can be used as an indication of a water phase transition.

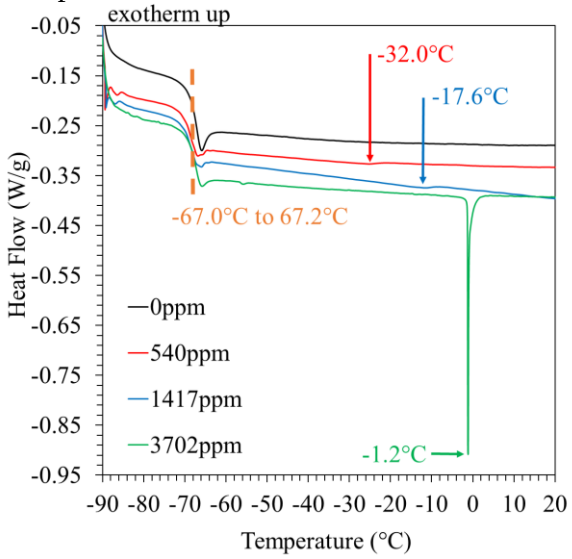

Figure 7: Overlay of DSC traces of four NP/water samples.

Interestingly, as the water concentration decreases from 3702 ppm to 540 ppm, the T_m peak changes shape to a very weak peak, which is barely detectable. This change in peak intensity is assumed to be related to the existence of a supernatant water layer. Accordingly, with the decrease in water concentration the T_m is greatly depressed from −1.15°C, −17.63°C, to −32.06°C. The three samples provided a basis for fitting a logarithmic trendline to extrapolate the T_m trend to 5800 ppm, the line $y = 16.059*\ln(x) - 133.45$ is well fit, with coefficient of determination $R^2 = 0.9984$, this line was used as the phase change between ice and liquid water in the phase diagram (Figure 8).

To verify the T_m as water rather than NP, the 3702 ppm sample was remade with the lid punctured. The sample was then run through a heat-cool-heat-cool cycle up to 110°C holding at 110°C for a 30-minute isotherm, allowing the majority of water to evaporate from the sample, for analysis purposes this sample is considered to be ~0 ppm of water, this sample showed no indication of a T_m, however the sample did display a T_g signal consitant with the other three runs. The ~0 ppm sample results renforced T_m as the result of water phase change as no T_m was observed after the drying process.

3.5 Phase Diagram

Combining the above experimental results, a temperature vs. concentration NP-water miscibility phase diagram was constructed and is presented in Figure 8. The results yielded six distinct phases; the physical states of the phases are expressed in colloidal terminology[6] on the diagram, however some states could be manifested as suspensions. Solid lines represent phase

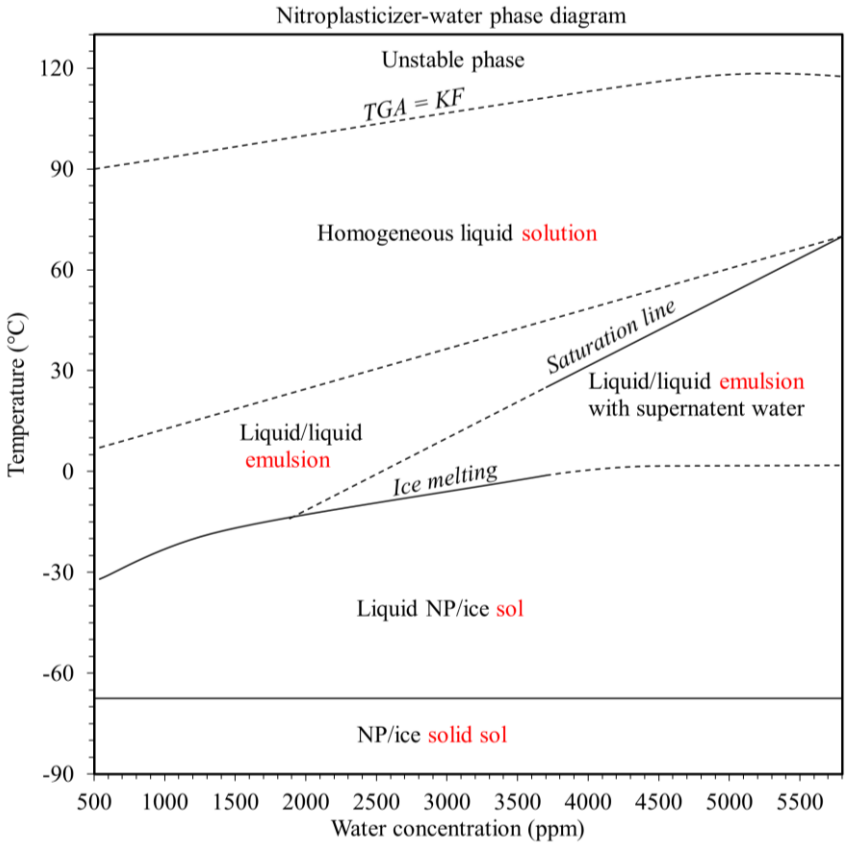

Figure 8: Temperature dependent phase diagram of NP-water miscibility, the boundaries were established by experimental results. Dashed line transitions represent transitions dependent on experimental conditions or extrapolations. States of matter are shown in red; all states are given in colloidal terminology as defined in US patent office Class 516.

transitions determined with minimal uncertainty, while narrow dashed lines represent measurements with considerable uncertainty, or extrapolated boundary sections.

The saturation line between liquid/liquid emulsion and liquid/liquid with supernatant water was determined by thermal equilibrated saturation of NP and KF titration, detailed in the KF and sample preparation sections of this paper. The transition from heterogeneous liquid/liquid emulsion to homogeneous liquid solution was evidenced by the variation in the water concentrations of the samples below 40°C are much higher than those above which were revealed in the KF and Near-IR measurments.

The transition from liquid NP/ice sol to solid sol is represented in the DSC data as the T_g, determined by heat-cool-heat conventional DSC, detailed in the DSC measurement section. The ice melting line and the transition from liquid/liquid emulsoin to liquid NP/ice sol are evidenced by the water T_m results from the DSC analysis.

The maximum temperature for water-NP interaction, the KF=TGA line, was determined by TGA compared with KF measurements. The line was placed at the points at which the mass loss by TGA closely matched the water concentration in the KF measurements. As some of the measurements showed considerable variability this line was dashed to express uncertainty.

4 Conclusion

By combining various techniques, phase diagram of NP-water miscibility was constructed. The results of this study created some clear boundaries for the NP-water temperature dependent phase diagram. The boundaries between NP/ice solid sol and liquid NP/ice sol around −67°C, between liquid/liquid emulsion and liquid Np/ice sol ranging from around −40°C to 0°C, and the liquid/liquid emulsion saturation creating a supernatant water layer are all clearly indicated by the experiments performed. The Near-IR data strongly correlate either loss or gain of peak areas with water concentration, particularly above 50°C.

The data clearly indicate, on heating from solid state, the water-NP solution passes through an emulsion state, before the solution becomes homogeneous. Above the homogeneity threshold, the (H_2O) in NP steadily increases with KF derived equation (H_2O) = 46.693*T + 2534.4 with least squares fit $R^2 = 0.9466$. Based on the TGA=KF test results it is expected the homogeneous/saturation line will extend all the way to up to 117°C at the maximum, at which point most water to boils out of NP. However, the material was only tested up to 70°C and expanding the phase diagram beyond its current limits would require extensive extrapolation.

Some phase boundaries are left more uncertain than others, the KF=TGA line, the broad transition from liquid/liquid emulsion to homogeneous solution, and ice melting line water all fall into the uncertain boundary category. Future work could be to build a stronger dataset for the placement of these boundaries. In the uncertain areas of the phase diagram, dashed boundaries are drawn to illustrate the general trend and express some degree of uncertainty. Despite these uncertain boundaries, many of the phase boundaries are evidenced by multipoint datasets and multiple testing techniques; firmly setting many boundaries in place by this study.

Acknowledgements

We thank Joseph Torres, Elisha Willis, Lindsey Kuettner, Caleb Van Buskirk and Brian Patterson for their input. This work was supported by the US Department of Energy through the Los Alamos National Laboratory Aging and Lifetimes Program. Los Alamos National Laboratory is operated by Los Alamos National Security, LLC, for the National Nuclear Security Administration of U.S. Department of Energy (Contract DEAC52-06NA25396).

References

1. (a) Salazar, M. R., Lightfoot, J. M., Russell, B. G., Rodin, W. A., McCarty, M., Wrobleski, D. A., Orler, E. B., Spieker, D. A., Assink, R. A., and Pack, R. T., Degradation of a Poly(ester urethane) Elastomer. III. Estane 5703 Hydrolysis: Experiments and Modeling. *Journal of Polymer Science: Part A: Polymer Chemistry* **2003,** *41*, 1136–1151; (b) Orler, E. B., Wrobleski, D. A. Cooke, D. W., Bennett, B. L. Smith, M.E. and Jahan, M. S., Thermal Aging of Nitroplasticized Estane 5703 No. LA-UR-02-1315. *Los Alamos National Laboratory* **2002**.

2. Idar, D. J., Thompson, D. G., Gray III, G. T. , Blumenthal, W. R., Cady, C. M., Peterson, P. D., Roemer, E. L., Wright, W. J., and Jacquez, B. J., Influence of Polymer Molecular Weight, Temperature, and Strain Rate on the Mechanical Properties of PBX 9501 *AIP Conference Proceedings* **2002,** *620* (1), 821.

3. (a) Salazar, M. R., Kress, J. D., Lightfoot, J. M., Russell B. G., Rodin W. A., and Woods, L, Experimental Study of the Oxidative Degradation of PBX 9501 and its Components. *Propellants, Explosives, Pyrotechnics* **2008,** *33* (3), 182-202; (b) Salazar, M. R., Kress, J. D., Lightfoot J. M., Russell, B. G., Rodin, W. A., and Woods, L., Low-temperature Oxidative Degradation of PBX 9501 and its Components Determined Via Molecular Weight Analysis of the Poly(ester urethane) Binder. *Polymer Degradation and Stability* **2009,** *94*, 2231-2240.

4. (a) Salazar, M. R., Thompson, S. L., Laintz, K. E. ,and Pack, R. T. , Degradation of a Poly(ester urethane) Elastomer. I. Absorption and Diffusion of Water in Estane 5703 and Related Polymers. *Journal of Polymer Science: Part B: Polymer Physics* **2002,** *40*, 181-191; (b) Salazar, M. R., and Pack R. T., Degradation of a Poly(ester urethane) Elastomer. II. Kinetic Modeling of the Hydrolysis of a Poly(butylene adipate). *Journal of Polymer Science: Part B: Polymer Physics* **2002,** *40*, 192-200; (c) Salazar, M. R., Thompson, S. L., Laintz, K. E., Meyer, T. O., and Pack R. T., Degradation of a Poly(ester urethane) Elastomer. IV. Sorption and Diffusion of Water in PBX 9501 and its Components. *Journal of Applied Polymer Science* **2007,** *105*, 1063-1076; (d) Yang, D., Pacheco, R., Edwards, S., Henderson, K., Wu, R., Labouriau, A., and Stark, P., Thermal Stability of a Eutectic Mixture of Bis(2,2-dinitropropyl) Acetal and Formal: Part A. Degridation Mechanisisms in Air and Under Nitrogen Atmosphere. *Polymer Degradation and Stability* **2016,** *129*, 380-398; (e) Yang, D., Pacheco, R., Edwards, S., Henderson, K., Wu, R., Labouriau, A., and Stark, P., Thermal Stability of a Eutectic Mixture of Bis(2,2-dinitropropyl) Acetal and Formal: Part B. Degradation Mechanisms Under Water and High Humidity Environments. *Polymer Degradation and Stability* **2016,** *130*, 338-347; (f) Yang, D., Torres, J., Henderson, K., Cluff, K., Adams, J., Edgar, A. *Stability of Naturally Aged Nitroplasticizer*; Los Alamos National Laboratory Los Alamos National Laboratory 2018; p 17.

5. Rebagay, T. V., Cash, R. J., Dodd, D. A., Meacham, J. E., & Narquis, C. T., FTIR fiber optic methods for the analysis of Hanford Site waste (No. WHC-SA-2894; CONF-9506234-1). *Westinghouse Hanford Co., Richland, WA (United States).* **1995**.

6. Class 516: Colloid Systems and Wetting Agents; Subcombinations Thereof; Process of Making, Stabilizing, Breaking, or Inhibiting. Office, U. S. P. a. T., Ed. Office of Classification Support (Office of Patent Classification): Reference Tools Project, 2007; p 171.

Appendix A : Nitric acid dilution table with TGA results.

Sample Name	8.7% HNO_3 solution		DI Water		(HNO_3) (%)	First derivative maximum TGA
	Density	1.413	Density	1.000		
	Mass (g)	Volume (mL)	Mass (g)	Volume (mL)		
1:0	1.0000	1.4130	0.0000	0.0000	70.0%	82.71
3:2	1.2790	1.8072	0.5358	0.5358	53.9%	88.03
1:1	0.6066	0.8571	0.7033	0.7033	38.5%	89.15
1:2	0.5176	0.7314	1.0944	1.0944	28.0%	88.96
1:3	0.2617	0.3698	0.8062	0.8062	22.0%	88.39
1:4	0.2891	0.4085	1.1098	1.1098	18.8%	86.55
1:5	0.2078	0.2936	1.0622	1.0622	15.2%	88.57
1:6	0.2563	0.3622	1.5868	1.5868	13.0%	87.91
1:8	0.1203	0.1700	1.0450	1.0450	9.79%	89.50
1:10	0.5029	0.7106	5.0504	5.0504	8.63%	85.48
1:12	0.1129	0.1595	1.2575	1.2575	7.88%	82.26
Sample Name	1:10 HNO_3 solution		DI Water		(HNO_3) (%)	First derivative maximum TGA
	Density	1.0259	Density	1.0000		
	Mass (g)	Volume (mL)	Mass (g)	Volume (mL)		
A:1	0.6069	0.8575	0.6360	0.6360	4.96%	79.02
A:5	0.2158	0.3049	1.0649	1.0649	1.92%	77.71
A:10	0.0990	0.1399	1.0430	1.0430	1.02%	80.04
A:20	0.0735	0.1039	1.1062	1.1062	0.741%	79.22
A:30	0.0397	0.0561	1.1262	1.1262	0.401%	77.94
A:40	0.0250	0.0353	1.0121	1.0121	0.291%	83.25
A:60	0.0172	0.0243	1.0443	1.0443	0.196%	78.87
A:80	0.0186	0.0263	1.3585	1.3585	0.164%	82.10
A:100	0.0076	0.0107	0.9775	0.9775	0.0938%	86.93
DI	1.0076	0.0000	1.0000	1.0000	0%	78.75

Appendix B: Preliminary work performed to create NP/water standards and to develop the methodology using KF titration water concentration in NP.

Standard vol.(mL)	water (ppm)	% diff (mean from 980ppm ideal)
0.8 to 1.0	979.74	0.026534
0.5	977.47	0.258838
0.4	989.37	0.951236
0.3	993.97	1.415086
0.2	982.77	0.281914
0.1	996.57	1.676307

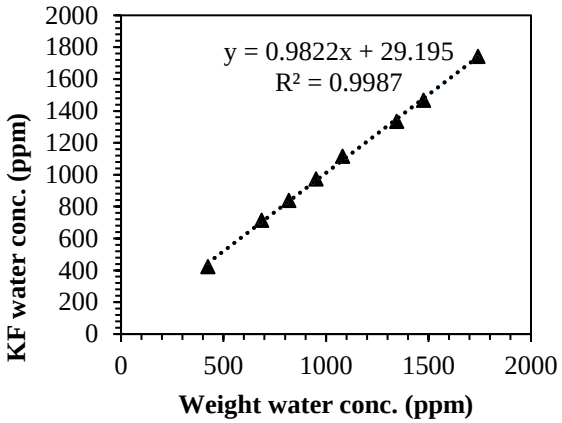

The plot above compares the water concentrations obtained from the KF measurement and the weight measurement for eight NP/water samples. The water concentrations of dry NP (424 ppm) and wet NP (1742 ppm) were determined by the KF measurement, the water concentrations in the other six samples were determined by changing the mixing weight ratios of the dry and wet NP samples. Later the KF measurement was carried out to validate their water concentrations. Clearly, the agreement between the weight and KF measurements is excellent, which confirms the KF method for the NP measurement is reliable.

KF analysis of NP standards and NP samples heated in a water bath

1. Use method “NP” on KF Titrator, or check the method is selected by pressing the “task” button
2. Use the “ start drift” button in the lower right of the display panel to determine average drift – record drift average given at the end of the determination
3. Analyze three replicates of 100ppm (1mL/analysis) and 1000ppm (0.3mL/analysis) standards, excess standard may be kept in HPLC 1.5mL vials capped and wrapped in parafilm
4. In a 1 mL syringe with 80x0.8mm needle, draw 0.9mL NP,

a. For standards drawing is made less difficult by removing the needle while drawing and replacing it to weigh and inject
b. For samples heated in a water bath draw from the NP container without removing form the water bath, doing so will require the needle be attached, be careful to not draw any supernatant water along with the NP

5. Place 80mL beaker on balance, stand/lean needle in the beaker ensuring the needle tip does not touch the glass doors or walls around the balance – tare balance with beaker, syringe, needle and contents
6. The drift is continuously monitor on the KF display, when the drift value displayed above the “start determination” is <1.5ug/min the determination can be started – press “start determination”, record injection number
7. Take the syringe from the beaker, leaving the beaker on the balance, inject ~0.3mL of NP through septa on top of the injection port of the KF, when titration is triggered the screen on the KF changes to the “enter mass” screen

8. When the titration has triggered replace the syringe/needle to the beaker still in the balance – record the mass loss, enter mass on the Titrator, press enter to begin titration
9. Titration will begin and a water determination will be made in ppm – record determined water, press enter, record current drift value
10. Tare balance and repeat steps 5-9 until 3 replicate NP aliquots have been analyzed
11. For NP samples heated in a water bath draw an additional 0.5mL NP and aliquot to a GPC vial for later analysis.

Appendix C: complete data set for KF titration and FTIR analysis. *) Integration range for inert sample is 5354-5207 cm^{-1} and 7182-7068 cm^{-1})

Date	Sample name	Cell Temp. (°C)	Integration area between 5423-4975 (cm^{-1}) *	Average area between 5423-4975 (cm^{-1})	Integration area between 7700-6500 (cm^{-1}) *	Average area between 7700-6500 (cm^{-1})	(H_2O) (ppm) KFT
020118	Inert 35C a	35	1.027		13.295		540.2
020118	Inert 35C b	35	1.031	1.029	13.292	13.2935	540.2
020118	Inert 40C a	40	0.844		13.387		540.2
020118	Inert 40C b	40	0.911	0.8775	13.329	13.358	540.2
020118	Inert 45C a	45	0.853		13.332		540.2
020118	Inert 45C b	45	0.897	0.875	13.368	13.35	540.2
020118	Inert 55C a	55	0.956		13.119		540.2
020118	Inert 55C b	55	0.958	0.957	13.14	13.1295	540.2
020118	Inert 60C a	60	0.927		13.038		540.2
020118	Inert 60C b	60	0.926	0.9265	13.089	13.0635	540.2
020118	Inert 65C a	65	0.891		13.176		540.2
020118	Inert 65C b	65	0.893	0.892	13.104	13.14	540.2
020118	Inert 70C a	70	0.865		13.241		540.2
020118	Inert 70C b	70	0.873	0.869	13.22	13.2305	540.2
031418	NP_25_27,7_1a	27.7	6.154		15.7090		4483.5
031418	NP_25_27,7_1b	27.7	6.145		15.5590		4483.5
031418	NP_25_27,7_2a	27.7	6.134		15.6470		4483.5
031418	NP_25_27,7_2b	27.7	6.100	6.1329	15.5130	15.607	4483.5
031418	NP_25_32,2_1a	32.2	6.427		15.8120		4483.5
031418	NP_25_32,2_1b	32.2	6.431		15.8310		4483.5
031418	NP_25_32,2_2a	32.2	6.503		15.8860		4483.5
031418	NP_25_32,2_2b	32.2	6.463	6.456	15.8680	15.84925	4483.5
031418	NP_25_34,7_1a	34.7	6.574		15.9510		4483.5
031418	NP_25_34,7_1b	34.7	6.568		15.8740		4483.5
031418	NP_25_34,7_2a	34.7	6.614		15.9610		4483.5
031418	NP_25_34,7_2b	34.7	6.572		15.9580		4483.5

031418	NP_25_34,7_3a	34.7	6.628	6.5912	15.9260	15.934	4483.5
031418	NP_25_40,0_1a	40	6.689		15.9890		4483.5
031418	NP_25_40,0_1b	40	6.685		16.0150		4483.5
031418	NP_25_40,0_2a	40	6.706		16.0390		4483.5
031418	NP_25_40,0_2b	40	6.688	6.692	15.9740	16.00425	4483.5
031418	NP_25_44,9_1a	44.9	6.634		16.0230		4483.5
031418	NP_25_44,9_1b	44.9	6.656		15.9560		4483.5
031418	NP_25_44,9_2a	44.9	6.656		15.8140		4483.5
031418	NP_25_44,9_2b	44.9	6.626	6.643	15.7640	15.88925	4483.5
031418	NP_25_49,9_1a	49.9	6.547		15.7420		4483.5
031418	NP_25_49,9_1b	49.9	6.550		15.7990		4483.5
031418	NP_25_49,9_2a	49.9	6.612		16.0000		4483.5
031418	NP_25_49,9_2b	49.9	6.602	6.57775	16.0120	15.88825	4483.5
031418	NP_25_55,0_1a	55	6.537		16.0220		4483.5
031418	NP_25_55,0_1b	55	6.532		15.9500		4483.5
031418	NP_25_55,0_2a	55	6.472	6.53575	15.5070	15.87275	4483.5
031418	NP_25_59,7_2b	55	6.432		15.0490		4483.5
031418	NP_25_59,7_1a	59.7	6.351		15.4250		4483.5
031418	NP_25_59,7_1b	59.7	6.364		16.0310		4483.5
031418	NP_25_59,7_2a	59.7	6.530	6.41925	16.0000	15.62625	4483.5
031418	NP_25_65,0_1a	65	6.472		15.9750		4483.5
031418	NP_25_65,0_1b	65	6.475		15.9750		4483.5
031418	NP_25_65,0_2a	65	6.340		15.3160		4483.5
031418	NP_25_65,0_2b	65	6.299	6.3965	15.3540	15.655	4483.5
031418	NP_25_70_1a	70	6.264		15.3070		4483.5
031418	NP_25_70_1b	70	6.263		15.3020		4483.5
031418	NP_25_70_2a	70	6.502		16.0310		4483.5
031418	NP_25_70_2b	70	6.452	6.37025	16.0080	15.662	4483.5
031918	NP_70_26,6_a	26.6	6.035		15.3380		5776.9
031918	NP_70_26,8_b	26.8	6.096		15.4220		5776.9
031918	NP_70_26,8_p2_a	26.8	6.068		15.4230		5776.9
031918	NP_70_26,8_p2_b	26.8	6.043	6.06055	15.3640	15.38675	5776.9
031918	NP_70_29,7_p1_a	29.7	6.253		15.4840		5776.9
031918	NP_70_29,7_p1_b	29.7	6.252		15.4540		5776.9
031918	NP_70_29,7_p2_a	29.7	6.233		15.5640		5776.9
031918	NP_70_29,7_p2_b	29.7	6.243	6.245325	15.5970	15.52475	5776.9
031918	NP_70_34,2_p1_a	34.2	6.673		15.6350		5776.9
031918	NP_70_34,2_p1_b	34.2	6.663		15.7320		5776.9
031918	NP_70_34,4_p2_a	34.4	6.670		15.7290		5776.9
031918	NP_70_34,7_p2_b	34.7	6.660	6.6665	15.6880	15.696	5776.9
031918	NP_70_40,1_p1_a	40.1	7.204		15.9600		5776.9

031918	NP_70_40,1_p1_b	40.1	7.187		16.0440		5776.9
031918	NP_70_40,1_p2_a	40.1	7.240		15.9920		5776.9
031918	NP_70_40,1_p2_b	40.1	7.243	7.2185	16.0060	16.0005	5776.9
031918	NP_70_45,1_p1_a	45.1	7.572		16.2090		5776.9
031918	NP_70_45,1_p1_b	45.1	7.576		16.2350		5776.9
031918	NP_70_45,1_p2_a	45.1	7.546		16.1710		5776.9
031918	NP_70_45,1_p2_b	45.1	7.560	7.5635	16.2300	16.21125	5776.9
031918	NP_70_49,9_p1_a	49.9	7.703		16.3070		5776.9
031918	NP_70_50,0_p2_a	50	7.809		16.3360		5776.9
031918	NP_70_50,0_p2_b	50	7.814	7.775333333	16.3220	16.3216666	5776.9
031918	NP_70_54,9_p1_a	54.9	7.714		16.3430		5776.9
031918	NP_70_54,9_p1_b	54.9	7.700		16.3360		5776.9
031918	NP_70_54,9_p2_a	54.9	7.785		16.3540		5776.9
031918	NP_70_54,9_p2_b	54.9	7.701	7.725	16.3020	16.33375	5776.9
031918	NP_70_59,8_p1_a	59.8	7.777		16.3680		5776.9
031918	NP_70_59,8_p1_b	59.8	7.776		16.3530		5776.9
031918	NP_70_59,8_p2_a	59.8	7.637		16.2810		5776.9
031918	NP_70_59,8_p2_b	59.8	7.637	7.70675	16.3130	16.32875	5776.9
031918	NP_70_65,0_p1_a	65	7.770		16.3810		5776.9
031918	NP_70_65,0_p1_b	65	7.824		16.4150		5776.9
031918	NP_70_65,0_p2_a	65	7.621		16.3240		5776.9
031918	NP_70_65,0_p2_b	65	7.624	7.70975	16.3580	16.3695	5776.9
031918	NP_70_70,0_p1_a	70	7.634		16.3900		5776.9
031918	NP_70_70,0_p1_b	70	7.633		16.3890		5776.9
031918	NP_70_70,0_p2_a	70	7.888		16.4480		5776.9
031918	NP_70_70,0_p2_b	70	7.881	7.759	16.5050	16.433	5776.9